PROJECT REPORT

On

SYNTHESIS AND CHARACTERIZATION OF Zn^{2+} DOPED CELLULOSE AEROGEL FROM ORANGE PEEL WASTE FOR OIL SPILL REMEDIATION

Submitted by

DEVIKA G
(AB23CHE021)

In partial fulfillment for the award of the

Bachelor's Degree in Chemistry

DEPARTMENT OF CHEMISTRY AND CENTRE FOR RESEARCH

ST. TERESA'S COLLEGE (AUTONOMOUS)
ERNAKULAM

2025-2026

DEPARTMENT OF CHEMISTRY AND CENTRE FOR RESEARCH

ST. TERESA'S COLLEGE (AUTONOMOUS)

ERNAKULAM

B.Sc. CHEMISTRY PROJECT REPORT

Name : DEVIKA G
Register Number : AB23CHE021
Year of Work : 2025-2026

This is to certify that the project **"SYNTHESIS AND CHARACTERIZATION OF Zn^{2+} DOPED CELLULOSE AEROGEL FROM ORANGE PEEL WASTE FOR OIL SPILL REMEDIATION"** is the work done by **DEVIKA G.**

Dr. Saritha Chandran A
Head of the Department

Dr. Raichel Mary Lopez
Staff-member in charge

Submitted to the Examination of Bachelor's Degree in Chemistry

Date: 10/04/26

Examiners: SENU DEVAKY KUTTY

DEPARTMENT OF CHEMISTRY AND CENTRE FOR RESEARCH

ST. TERESA'S COLLEGE (AUTONOMOUS)

ERNAKULAM

CERTIFICATE

This is to certify that the project work entitled "**SYNTHESIS AND CHARACTERIZATION OF Zn^{2+} DOPED CELLULOSE AEROGEL FROM ORANGE PEEL WASTE FOR OIL SPILL REMEDIATION**" is the work done by **DEVIKA G** under my guidance in the partial fulfilment of the award of the Degree of Bachelor of Science in Chemistry at St. Teresa's College (Autonomous), Ernakulam affiliated to Mahatma Gandhi University, Kottayam.

Dr. Raichel Mary Lopez
Project Guide
Assistant Professor
Department of Chemistry and Centre for Research
St. Teresa's College(Autonomous), Ernakulam

DECLARATION

I hereby declare that the project work entitled **"SYNTHESIS AND CHARACTERIZATION OF Zn^{2+} DOPED CELLULOSE AEROGEL FROM ORANGE PEEL WASTE FOR OIL SPILL REMEDIATION"** submitted to Department of Chemistry and Centre for Research, St. Teresa's College (Autonomous) affiliated to Mahatma Gandhi University, Kottayam, is a record of an original work done by me under the guidance of **Dr. RAICHEL MARY LOPEZ, Assistant professor,** Department of Chemistry and Centre for Research, St. Teresa's College (Autonomous), Ernakulam and this project work is submitted in the partial fulfilment of the requirements for the award of the Degree of Bachelor of Science in Chemistry.

DEVIKA G

Acknowledgements

First of all, I would like to thank Almighty God for the successful completion of this project.

I express my sincere gratitude to my project guide Dr. Raichel Mary Lopez, Assistant professor, St. Teresa's College (Autonomous), Ernakulam, for the valuable guidance, encouragement and support throughout the completion of this project.

I would like to extend my heartfelt thanks to Dr. Saritha Chandran A., Head of the Department of Chemistry and Centre for Research, St. Teresa's College (Autonomous), Ernakulam, for the continuous motivation and academic support.

I also express my respectful gratitude to Dr. Anu Joseph, Principal, St. Teresa's College (Autonomous), Ernakulam, for providing the necessary facilities and a supportive environment to carry out this work. I gratefully acknowledge the management of the institution for the infrastructure and resources provided.

I express my sincere thanks to all teachers of the Chemistry Department, for their constant guidance and support throughout the academic year. I also gratefully acknowledge the help and cooperation of the non-teaching staffs of the department during the Chemistry Lab hours and project hours. I heartily thank STIC (CUSAT), School of Environmental Studies and Amrita School of Nanoscience and Molecular Medicine for providing all

the assistance needed for the characterization of the samples within the time limit.

Finally, I thank my dear friends and families for their encouragement, understanding and moral support throughout the project.

DEVIKA G

Contents

Chapter 1

Introduction

1.1 AGRICULTURAL WASTE UPCYCLING

In today's world, due to the increasing scarcity of oil resources and serious environmental pollution problems caused by petroleum-based polymers, biodegradable, inexpensive, and non-toxic natural polymer materials have attracted considerable attention from researchers, corporations, and governments. The escalating global demand for sustainable materials necessitates the utilization of renewable resources and the valorization of waste biomass. Lignocellulose agricultural waste, particularly orange peel (OP), represents a substantial, readily available, and inexpensive source of cellulose. Annually, millions of tons of orange peel are generated by the juice industry, posing a significant waste disposal challenge. Transforming this waste into high-value materials aligns perfectly with the principles of the circular economy. *(1)*

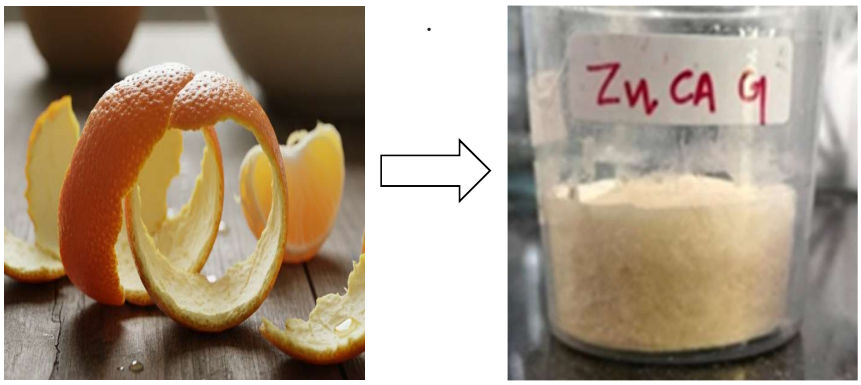

FIG. 1.1 ORANGE PEEL TO AEROGEL

Upcycling food losses and waste in their integrity [or "bulk" waste]-i.e., without extracting individual components-into bio-based materials has emerged as a promising strategy within the Green Manufacturing and Engineering approach to reduce the use of harsh chemicals, waste generation, and save processing operations, time and energy *(2)*.

1.2 **ORANGE PEEL**

Citrus fruits, including oranges, grapefruits, and lemons, are among the most widely consumed fruits across the globe, mainly due to their pleasant flavor and significant nutritional value. In addition to being rich sources of vitamins and minerals, these fruits contain a wide range of bioactive phytochemicals that are known to provide protective effects against several gastrointestinal disorders, including gastric, oesophageal, and colorectal diseases *(3)*.

Similar to other plant-derived materials and natural lignocellulosic resources, citrus fruits are structurally composed of three major organic constituents: cellulose, hemicellulose, and lignin. Among these components, cellulose is the most prominent and is primarily found in the cell walls of plants. It represents the most abundant renewable natural polymer on Earth and plays a vital role in maintaining the structural integrity of plant tissues.

Cellulose is a biodegradable biopolymer that can be naturally decomposed by microorganisms present in the soil, ultimately breaking down into environmentally harmless products such as carbon dioxide and water. From a molecular perspective, cellulose is a high-molecular-weight polymer consisting of repeating units of D-glucose that are linked together through

β-1,4-glycosidic bonds. These glucose chains are held together mainly by extensive hydrogen bonding, which contributes to the formation of a highly ordered and crystalline structure.

Despite this crystalline arrangement, cellulose is not entirely uniform in structure. It also contains non-crystalline or amorphous regions, which arise due to the presence and orientation of hydroxyl groups within the glucose units. These amorphous regions influence the physical and chemical behavior of cellulose and play an important role in its reactivity and interaction with other substances *(4)*.

FIG. 1.2 ORANGE PEEL

1.3 **CELLULOSE**

Cellulose is the most abundant natural polymer found on Earth and plays a fundamental role in the structure of plant-based materials. From a structural standpoint, cellulose is a linear polymer composed of repeating D-glucose units that are interconnected through 1,4-β-glycosidic bonds.

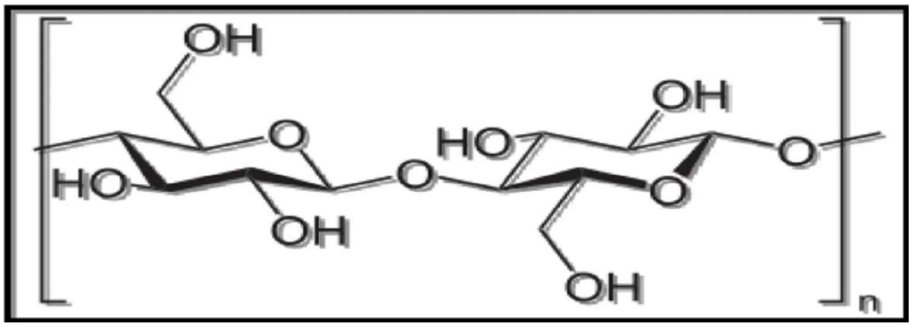

FIG. 1.3 STRUCTURE OF CELLULOSE

Owing to this molecular arrangement, cellulose exhibits a unique combination of properties that clearly distinguish it from conventional petroleum-based polymers. These properties include excellent biocompatibility, biodegradability, high thermal and chemical stability, and low production cost, making cellulose an environmentally sustainable and economically attractive material.

The use of cellulose in industrial applications has a long history dating back thousands of years. Traditional products such as paper, cardboard, textiles, and construction materials have relied heavily on cellulose for their structural strength and layered architecture. However, in these conventional applications, only basic characteristics of cellulose such as its rigidity and multi-layer structure have been utilized. As a result, these materials often fall short of meeting modern demands for advanced functionality, long-term durability, and structural uniformity that are required for next-generation materials in the 21st century.

In recent years, increased research into the physical and chemical behavior of cellulose has led to the development of a wide range of environmentally friendly and functional cellulose-based materials. These include cellulose

fibres, thin films, hydrogels, aerogels, and various cellulose-based composite materials. Among these, cellulose aerogels have attracted particular attention due to their ability to retain the inherent advantages of cellulose, such as renewability, biocompatibility, and biodegradability of cellulose, while also exhibiting exceptional properties including extremely low density, high porosity, and a large specific surface area. Because of this unique combination of characteristics, cellulose aerogels are considered one of the most promising advanced materials for applications in the 21st century *(5)*.

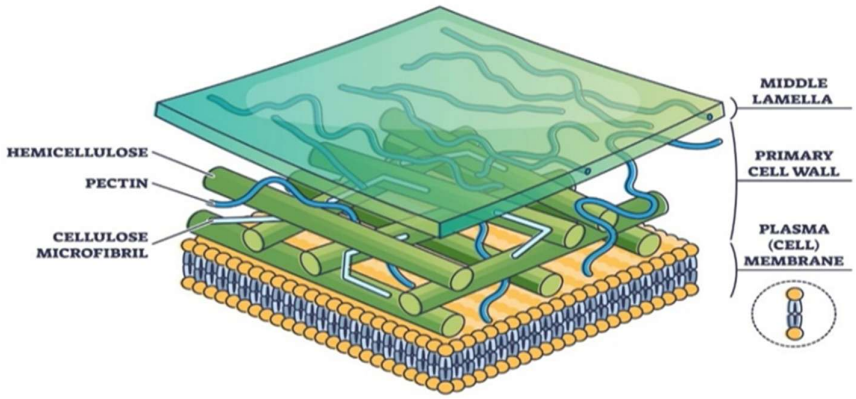

FIG.1.4 CELL WALL STRUCTURE

1.3.1 **SOURCE OF CELLULOSE**

Cellulose, the world's most abundant natural biopolymer, is primarily sourced from the cell walls of vascular plants where it forms the crucial structural component. The major commercial sources include wood pulp, derived from both softwoods (yielding longer, stronger fibers) and hardwoods (providing shorter, smoother fibers), which dominate the paper

industry. High-purity cotton fibers and linters represent the purest cellulosic source, essential for producing high-grade derivatives like nitrocellulose and acetates. Additionally, various agricultural residues such as wheat straw and bagasse, along with bast fibers like jute and flax, serve as inexpensive, sustainable, but often challenging lignocellulosic sources. Beyond the plant kingdom, specialized forms of cellulose are produced by non-plant organisms; specifically, certain strains of bacteria, such as Gluconacetobacter xylinum, synthesize bacterial cellulose, which is characterized by its unique nanoscale structure, exceptional purity, and high crystallinity, making it highly valuable for advanced biomedical applications. Furthermore, the cell walls of certain algae and the protective tunic of marine invertebrates like tunicates yield cellulose with superior crystalline perfection, offering niche sources for the production of highly crystalline nanomaterials like cellulose nanocrystals (CNC). Thus, the diversity of sources ensures a robust supply chain catering to applications from bulk paper products to high-technology biomaterials *(6)*.

1.4 **AEROGEL**

Aerogel is a type of special porous material with excellent physical and chemical properties, such as low density (0.003–0.500 $g \cdot cm^{-3}$), high porosity (80~99.8%), large specific surface area (100~1600 m^2/g), and adequate surface chemical activities. Technologies with the potential to be improved by aerogel include those used in the areas of optoelectronics, adsorption catalysis, sound insulation, medical materials, aerospace materials, and many other fields. However, the mechanical properties of silica aerogels are poor, and the precursors of synthetic polymer-based aerogels are toxic and non-degradable. Coupled with their high cost of

preparation, these factors have significantly restricted the application of aerogels *(5)*.

The specific surface area (10-975 m^2/g), porosity (84.0-99.9%), and density (0.0005-0.35 $g \cdot cm^{-3}$) of cellulose aerogels are comparable to those of traditional silica aerogels and synthetic polymer aerogels, but cellulose aerogels have a higher compressive strength (5.2 KPa–16.67 MPa) and better biodegradability. Therefore, cellulose aerogels are a type of environmentally-friendly and multi-functional new material that has great potential in the application of adsorption and oil/water separation, heat insulation, biomedical materials, and many other areas *(5)*.

1.5 **ZINC OXIDE AS DOPANT (ZnO)**

ZnO is one of the compounds exhibiting amphoteric nature, which present as $Zn(OH)_4^{2-}$ species in strong alkaline solutions. This $Zn(OH)_4^{2-}$ species can form stronger hydrogen bonds with cellulose than that of hydrated NaOH system, which leads to the improvement of cellulose dissolution. Further, the addition of ZnO not only improves the dissolution of cellulose but also is reported to act as a stabilizer against the gelation of cellulose *(7)*.

1.6 **APPLICATIONS OF CELLULOSE AEROGELS**

1.6.1 **ENVIRONMENTAL REMEDIATION AND OIL/ WATER SEPERATION**

A major application of cellulose aerogels is in environmental clean-up, particularly for separating oil/organic solvents from water, crucial for treating oil spills and industrial wastewater. Native cellulose is hydrophilic, meaning it attracts water, but chemical surface modification-typically

through methods like chemical vapor deposition using silanes (e.g., MTMS or HTMS)-converts the aerogel into a superhydrophobic and super oleophilic material. This modified material strongly repels water (water contact angle > 150°) but selectively adsorbs oil, allowing it to function as a highly efficient, high-capacity, and reusable sorbent. Their low density allows them to float on the water surface, making retrieval easy, and their open-pore structure contributes to exceptional adsorption capacities, often exceeding 100 g/g *(8)*.

1.6.2 **DRUG DELIVERY SYSTEMS**

Cellulose aerogels are exceptional carriers for controlled drug delivery due to their non-toxicity, biodegradability, and high pore volume. The hierarchical porous structure allows for high drug loading capacity, as the active pharmaceutical ingredient (API) can be adsorbed both on the large internal surface area and within the macropores of the aerogel matrix. Once administered, the aerogel's porous network controls the release kinetics of the loaded drug, allowing for sustained or triggered release. By modifying the surface chemistry of the cellulose, researchers can achieve pH- or temperature-responsive release profiles, tailoring the system to specific biological environments to enhance drug bioavailability and reduce dosing frequency *(5)*.

1.6.3 **THERMAL AND ACOUSTIC INSULATION**

Cellulose aerogels are highly effective thermal insulators, offering a sustainable alternative to fossil-fuel-based materials, primarily for building insulation. Their low thermal conductivity (λ) is achieved by utilizing their ultra-high porosity (often > 95%) and nanoporous structure. This structure confines air within the pores, suppressing two main modes of heat transfer:

convection and conduction. The pore sizes are engineered to be smaller than the mean free path of air molecules (a phenomenon known as the Knudsen effect), which significantly decreases the gaseous phase contribution to heat transfer, allowing thermal conductivities to drop below 0.025 $W \cdot m^{-1} \cdot K^{-1}$. Furthermore, the composite aerogels also exhibit good sound absorption coefficients, making them useful for acoustic dampening *(5)*.

1.6.4 CARBON CAPTURE AND UTILIZATION (CCU)

Cellulose aerogels are emerging as promising, green adsorbents for capturing carbon dioxide (CO_2), a critical step in mitigating global climate change. Due to their high porosity and large surface area, the aerogels provide numerous active sites for CO_2 adsorption. Native cellulose is often modified through functionalization with nitrogen-containing groups (e.g., amines), which react chemically with CO_2 (chemisorption). This modification significantly improves the material's adsorption performance, making them highly relevant for applications like post-combustion CO_2 capture *(9)*.

1.6.5 ELECTROMAGNETIC(EM) SHIELDING MATERIALS

Functionalized cellulose aerogels are being developed as lightweight, high-performance materials for Electromagnetic Interference (EMI) shielding, crucial for protecting sensitive electronics and personnel from EM radiation. Cellulose itself is an insulator, but aerogels can be made conductive by incorporating carbon-based materials (like Carbon Nanotubes, CNTs, or Graphene) or conductive nanoparticles. The resulting conductive composite aerogel creates a continuous 3D conductive network that facilitates the absorption and dissipation of electromagnetic waves through mechanisms like multiple reflections within the hierarchical porous

structure and interfacial polarization. This leads to high EMI shielding effectiveness (SE) values with an absorption-dominated attenuation mechanism, offering superior performance compared to traditional dense metal shields on a weight-specific basis*(10)*.

1.6.6 **ADVANCED SENSING AND BIOSENSORS**

Cellulose aerogels offer an ideal platform for constructing highly sensitive and selective sensors, including biosensors, gas sensors, and strain/pressure sensors. The aerogel matrix serves as a rigid, yet flexible, 3D scaffolding that can host sensing elements while offering excellent structural integrity. The high porosity allows for rapid analyte diffusion and large surface area interaction, improving sensitivity. Flexible cellulose aerogel-based composites can be fabricated into pressure and strain sensors for wearable electronics; the change in the aerogel's porous network under pressure translates into a measurable change in electrical conductivity *(11)*.

1.7 **SUMMARY OF EXISTING STUDIES ON AEROGELS DERIVED FROM AGRICUTURAL WASTES**

According to reports cellulose-based aerogels prepared by the freeze-drying method are among the most promising and studied aerogels for adsorption of contaminants *(10) -(14)* stated that aerogels derived from freeze-drying and carbonization processes showed good interconnected mesoporous structure, large specific area of 734.96 m^2/g needed for adsorption. Also, good structural morphology and adsorption capacities was derived from pineapple fiber and banana stem *(15)*. The summary of existing studies on agricultural wastes aerogels in Table 1 shows that significant number of agricultural wastes have been successfully modified as cellulose aerogels.

However, the results obtained from using waste biomass based cellulose aerogels particularly in contaminants remediation is variable due to factors such as hydrophilicity and need chemical modification, selective absorption of oil, and poor structural integrity especially in harsh or industrially contaminated environments *(16)*

Table 1. Review Table On Cellulose Aerogel

Waste material	**Preparation process**	**Density g/cm^3**	**Porosity %**	**Contact angle**	**Absorption capacities g/g**	**Application**	**Reference**
Banana leaf	Freeze drying	0.015		149^0	35-115	Adsorption of oil/organic solvents	*(17)*
Banana stem	Freeze drying + Pyrolysis			135^0	35	Thermal insulation	*(15)*
Pineapple leaf	Freeze drying	0.127 – 0.326	97-99			Thermal insulation	*(18)*
Pineapple leaf	Freeze drying	0.063 – 0.093	92-94			Thermal insulation	*(19)*
Pineapple leaf	Freeze drying	0.013-0.033	96-99	140^0	38	Adsorption of oil	*(19)*
Pineapple leaf + Cotton waste	Freeze drying	0.019-0.046	96			Thermal insulation	*(20)*
Peanut shell	Freeze drying + Carbonization		98	141^0	27-50	Adsorption of oil/organic solvents	*(21)*

Seaweed solid waste	Freeze drying + Carbonization			153^0	11-30	Adsorption of oil	*(22)*
Rice straw	Freeze drying	0.012	99.5	120^0	28-70	Adsorption of oil/organic solvents	*(23)*
Rice straw	Freeze drying	0.002-0.024	98.4-99.8	151^0	98-170	Adsorption of oil/organic solvents	*(24)*
Rice straw	Freeze drying	0.05-0.06	97	150^0	13	Thermal insulation	*(25)*
Bamboo powder + Wastepaper	Freeze drying	0.011		118^0-142^0	67-121	Adsorption of oil	*(26)*
Soybean stalk	Freeze drying		95-97		16-31	Adsorption of oil	*(27)*
Sugarcane bagasse	Freeze drying	0.016-0.122	91.9-98.9		98.8	Adsorption of oil/organic solvents	*(12)*
Sugarcane bagasse	Freeze drying	0.016-0.112	92-99		25	Adsorption of oil/organic solvents	*(25)*
Sugarcane bagasse	Freeze drying	0.012-0.108	92.9-99.2	140^0	23	Thermal insulation/oil adsorption	*(28)*
Sorghum stem	Freeze drying	0.146-0.167	90		19-30	Adsorption of dyes	*(29)*
White bamboo	Freeze drying	0.085-0.144	90-95	114^0-132^0	99.9	Adsorption of oil	*(10)*

Durian	Ultrasonic	0.003-0.012	99				*(30)*
Durian	Freeze drying	0.5				Super capacitor	*(12)*
Watermelon rind	Freeze drying + Pyrolysis		91-94	127^0	53.51-70.52	Adsorption/ energy storage	*(15)*
Pomelo	Freeze drying			128^0-135^0	5-36	Adsorption of organic pollutants and oil	*(14)*
Pomelo	Freeze drying + Carbonization	0.020	98	132^0	49.2-71.3	Adsorption of organic pollutants and oil	*(31)*
Pomelo	Freeze drying	0.18-0.23	80-87		1.7-3.9	Adsorption of organic pollutants and oil	*(13)*
Pomelo fruit peels + wastepaper	Freeze drying	0.611	99	139^0	24.48-34.97	Adsorption of oil	*(32)*
Coconut peat	Freeze drying		98		24.52	Adsorption of oil	*(33)*
Coconut fiber	Freeze drying + Carbonization	0.034-0.063	96-98		0.63-0.65	Adsorption of dyes	*(34)*
Cabbage	Freeze drying				>80	Adsorption of oil and organic solvent/ super capacitor	*(35)*

Grapefruit peels	Freeze drying	0.051		141^0	75-95	Adsorption of oil/organic solvents	*(36)*

1.8 OBJECTIVES

- Preparation of zinc doped cellulose aerogel from orange peel.
- Characterization of prepared zinc doped cellulose aerogel from orange peel by FTIR, XRD, SEM and EDAX.
- To evaluate the efficiency of the prepared sample towards oil sorption and other environmental applications.
- To compare the porosity development of Zn^{2+} doped cellulose aerogel with the raw cellulose aerogel

Chapter 2

Materials and Methods

This chapter gives a brief description of the materials and experimental procedures adopted for the present investigation.

2.1 MATERIALS AND REQUIREMENTS

- Orange peel
- Distilled water
- Sodium hydroxide
- Urea
- Sesame oil
- Zinc acetate
- Gelatin powder

2.2 APPARATUS REQUIRED

- Hot air oven
- Temperature control magnetic stirrer
- Grinder
- Freeze dryer

2.3 EXTRACTION OF CELLULOSE FROM ORANGE PEEL

i) **Preparation of powdered sample**

The orange peel was washed in distilled water and kept for oven dry for 2 days. The cellulose based material separately grinded and sieved in 300μm sieve was taken.

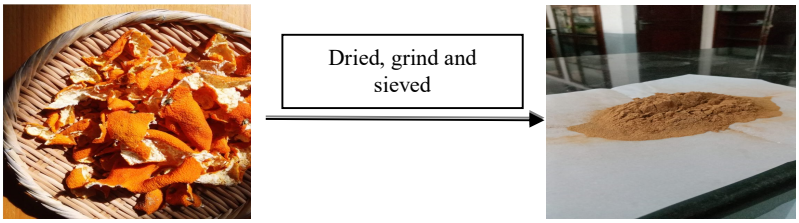

Fig.2.1. Preparation of powdered sample

ii) **Alkaline Pre-treatment and Washing**

A certain amount of grounded OPP (80–100 meshes) was immersed into a solution of 4 wt.% sodium hydroxide with a solid–liquid ratio of 1:10 and the mixture was kept at 40^0C for 6 h under magnetic stirring. After that, the product was filtered and thoroughly washed in distilled water until the filtrate was colorless and transparent (pH 7). The obtained material was dried at 60^0C for 24 h. The material was grinded and sieved. The obtained compound was named as CTOPP.

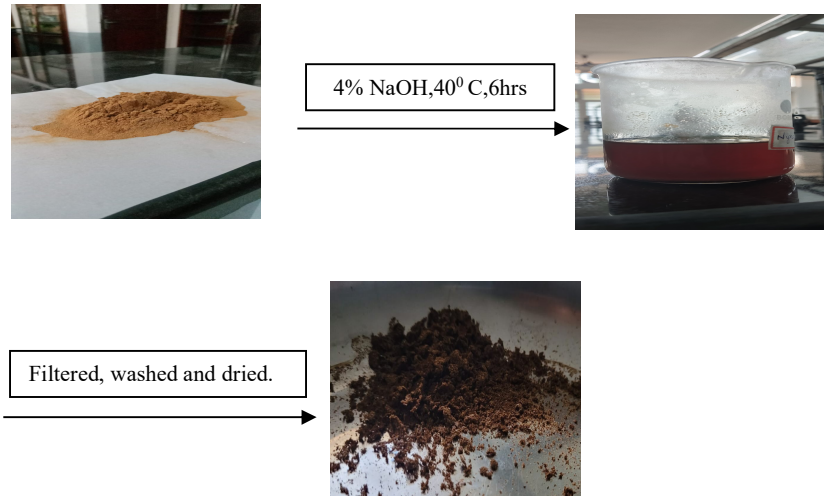

Fig.2.2. Alkaline Pre-treatment and Washing

2.4 PREPARATION OF AEROGEL-DISSOLUTION OF CELLULOSE, AEROGEL FORMATION AND FREEZE-DRYING.

i) **Dissolution and Initial Solution Preparation**

To the 1.5 g of CTOPP, 0.75g NaOH ,1.5g UREA,0.5g Zn $(COO)_2$ and 25 ml distilled water were stirred for 2hrs using magnetic stirrer.

ii) **Gelatin Introduction**

A gelatin solution was prepared by dissolving gelatin in distilled water under heating. The solution was then added to the previously obtained mixture stirred for an additional 1 hr.

iii) **Final Shaping and Drying**

The final mixture was allowed to cool, poured into molds, and subsequently frozen for frozen for 24 hrs. The frozen samples (Zn CA G) were then subjected to freeze-drying for 56 hrs. to obtain the final product.

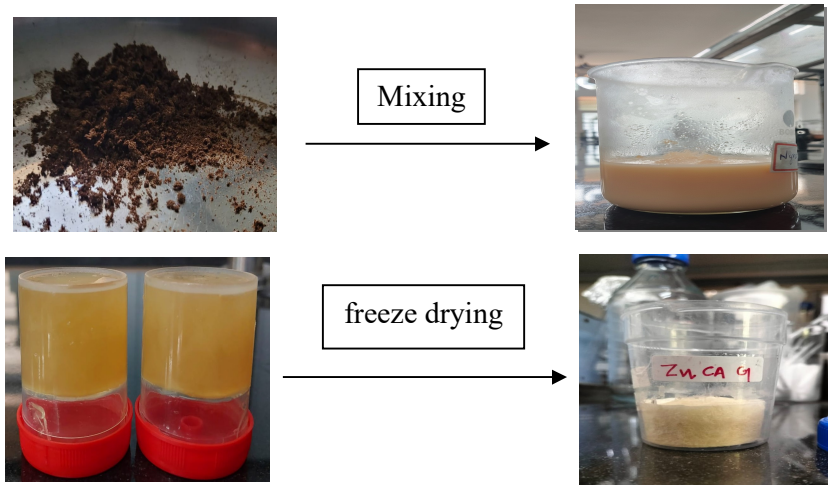

Fig.2.3. Preparation of aerogel includes dissolution and gelatin introduction and freeze-drying.

2.5 CHARACTERIZATION TECHNIQUES

The Zn^{2+}doped cellulose aerogel was characterized using X-Ray Diffraction (XRD), Fourier Transform Infrared Spectroscopy (FTIR), Scanning Electron Microscopy (SEM) and Energy Dispersive X-Ray analysis (EDAX). Oil adsorption capacity and oil removal efficiency was also evaluated.

2.5.1 X-RAY DIFFRACTION (XRD)

X-ray diffraction (XRD) is a powerful non-destructive technique for characterizing crystalline materials. It provides information on structures, phases, preferred crystal orientations (texture), and other structural parameters, such as average grain size, crystallinity, strain, and crystal defects. X-ray diffraction peaks are produced by constructive interference of a monochromatic beam of X-rays scattered at specific angles from each set of lattice planes in a sample. The peak intensities are determined by the distribution of atoms within the lattice. Consequently, the X-ray diffraction pattern is the fingerprint of periodic atomic arrangements in a given material. This review summarizes the scientific trends associated with the rapid development of the technique of X-ray diffraction over the past years pertaining to the field of pharmaceutical industry, forensic science, geological applications, microelectronics and glass industry, as well as in corrosion analysis. *(37)*

The Diffraction patterns of the carbon aerogel samples was obtained using a Bruker AXS-D8 Advance diffractometer using Cu-Kα (λ=1.5406 A^o) radiation at 40 kV and 30 mA, using continuous scan mode. The X-ray patterns were recorded in the scan range $2\theta=3^0$-80^0, at a scan rate of 1^0/min. The determination of XRD parameters were evaluated using Origin 8.0 software. The crystallinity index and the miller indices are also calculated.

The d- spacing of the planes of the sample was calculated using the Bragg's equation, $n\lambda = 2d\sin\theta$

It relates the wavelength(λ), order of diffraction(n), interlayer spacing(d) and angle of diffraction(θ).

The crystallinity index, CrI or the degree of crystallinity, was determined by Segal's method, using Equation

$$CrI = (I_{002} - I_{amr}) \times 100 / I_{002}$$

where I_{002} provides the maximum peak intensity value for the crystalline cellulose at about 2θ = 22.0° to 24.0° and I_{amr} gives the peak intensity of diffraction of the amorphous region at about 2θ = 18.0°.

2.5.2 FTIR ANALYSIS

Fourier-transform infrared spectroscopy is an analytical methodology used to analyse the structure of individual molecules, or the composition of molecular mixtures. FTIR spectroscopy uses modulated, mid-infrared energy (4000–400 cm^{-1}). The infrared light is absorbed at specific frequencies directly related to the atom-to-atom vibrational bond energies in the molecule or the crystal. When exposed to infrared radiation, sample molecules selectively absorb radiation of specific wavelengths which cause the change of dipole moment. Consequently, the vibrational energy levels of samples transfer from ground state to excited state. The frequency of the absorption peak is determined by the vibrational energy gap. The number of absorption peaks is related to the number of vibrational freedom of the molecule. The intensity of absorption peaks is related to the change of dipole moment and the possibility of the transition of energy levels.

As all the molecules contribute at different wavelengths depending on their chemical bonds, the adsorption or functionalization of clay minerals surfaces by surfactants and polymers can be directly observed on their FTIR spectra. *(38)*

The FTIR spectrum of the respective carbons was obtained by analysis on a Thermo Nicolet Avatar 370 over the frequency range of 4000–400 cm^{-1} by

placing the carbon samples on KBr pellets. The resolution of the instrument is 0–9 cm^{-1} with a signal–to–noise ratio 15000:1 and measured wavelength range 7800–375 cm^{-1}.

2.5.3 SCANNING ELECTRON MICROSCOPY (SEM)

Scanning electron microscopy (SEM) is a commonly used method to characterize membrane morphology. It scans the surface of the sample using a dense electron beam, converts the received signal into Gray-scale data, and displays it on the screen. Since the wavelength of the electron beam is much smaller than that of visible light, the resolution of the electron microscope is much higher than that of an optical microscope. The maximum magnification of the optical microscope is only approximately 1500 times, and the scanning microscope can magnify more than 10,000 times. The vacuum system in the instrument ensures the normal operation of the electron optical system and prevents contamination of the sample.

SEM can be combined with an X-ray spectrometer or X-ray energy spectrometer to comprehensively analyse the surface of the sample with element detection. If the sample has good conductivity, the surface does not need any treatment and can be observed directly. If it is a non-conductor, it needs to be coated with a metal film or carbon film to help the sample conduct electricity. The coating material is usually gold, palladium, or carbon. The carbon film is more suitable for X-ray microanalysis, mainly because carbon has a low atomic number, which can reduce X-ray absorption. To observe the cross section of the membrane sample, the sample may need to be brittle-fractured using liquid nitrogen to avoid deformation. In addition, water-containing samples can be observed by environmental scanning electron microscopy (ESEM), but water mist may cause a decrease in clarity.*(39)*

The surface morphology was evaluated using the Scanning Electron Microscope - JEOL Model JSM - 6390LV working at a high resolution of 3.0 nm in an accelerating voltage of 0.5 to 30 kV with a magnification of 5x to 300,000x. The

carbon samples were coated with gold using a sputter coating unit (model: JFC1600) prior to SEM analysis for 10 s at 10 mA.

2.5.4 ENERGY DISPERSIVE X-RAY ANALYSIS

Energy-dispersive X-ray spectroscopy, sometimes called energy-dispersive X-ray analysis or energy-dispersive X-ray microanalysis, is based on the measurement of the energy of characteristic X-ray emissions of excited specimens under study. To stimulate the emission, a high-energy beam of charged particles such as electrons or protons, or a beam of X-rays, is focused into the observable specimen. At rest, an atom within the sample contains a ground state (or unexcited electrons) in discrete energy levels or electron shells bound to the nucleus. The incident beam may excite an electron in an inner shell, ejecting it from the shell, while creating an electron hole that is filled by an electron from a higher-energy shell. The difference in energy between the higher-energy shell and the lower-energy shell may be released in the form of an X-ray. The number and energy of the X-rays emitted from a specimen can be measured by an energy-dispersive spectrometer that allows us to define the elemental composition of the specimen.*(40)*

Energy dispersive X-ray analysis (EDX) is performed in conjunction with SEM or TEM. It provides the elemental details of near surface elements of a sample and the overall positional mapping in it. Here a high energy electron beam ~ 10–20 keV is bombarded on a sample and X-rays emitted from the sample are collected by an energy dispersive spectrometer *(41)*

2.6 OIL ADSORPTION CAPACITY

The oil adsorption capacity (Q)was used to evaluate the efficiency of the aerogel template. The oil adsorption capacity was calculated as follow:*(42)*

$$Q=(W_1-W_0)/W_0$$

where W_1 = weight of the material after sorption

W_0= weight of the material before sorption

2.7 OIL REMOVAL EFFICIENCY

In order to know the oil removal capacity of the aerogel, the oil removal efficiency was calculated using equation:*(42)*

$$RE\ (\%) = (W_1 - W_0) \times 100 / W_1$$

where W_1 = weight of the material after sorption

W_0= weight of the material before sorption

Chapter 3

Results and discussion

3.1 X-RAY DIFFRACTION ANALYSIS

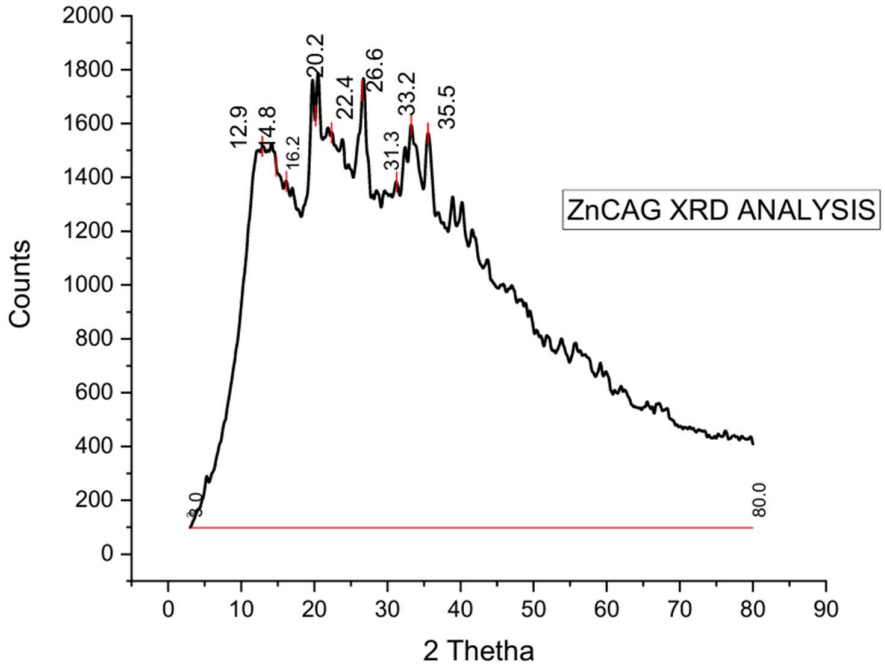

Fig 3.1. XRD spectrum of ZnCAG

The Fig 3.1 represents the XRD of ZnCAG. XRD analysis was carried out to determine the crystallinity index, in addition to the changes in the crystallinity and amorphous region of ZnCAG, in comparison with cellulose extracted from orange peel.

The diffraction peaks at 2θ = 14.0°, 16.5°, and 22.5° for (1 1 0), ($1\bar{1}$ 0), and (0 2 0) planes, respectively, are characteristic for cellulose I crystal, and

those at 2θ = 12.5°, 20.5°, and 22.1° for (1 1 0), (1$\bar{1}$ 0), and (0 2 0) planes, respectively, are signed to cellulose II crystal. However, weak peaks of cellulose I were also detected in the XRD pattern of cellulose II due to the incomplete transformation *(43)*. The prominent peaks coordinating the reflection surface (100), (002), (101), (102), (110), (103), (200), (112), (201), (004), and (202) reveal the ZnO particles. The sharp and narrow peaks of XRD patterns ensure good crystallinity, while the absence of any additional peaks ensures the absence of NPs*(44)*. The XRD peaks and the corresponding miller indices were given in the table (3.1)

Table 3.1. XRD Parameters Of ZnCAG

XRD Peaks	**Miller Indices(hkl)**	**d-spacing**
12.9	(1 10)	0.69 nm
14.8	(1 1 0)	0.60 nm
16.2	(1$\bar{1}$ 0)	0.55 nm
20.2	(1$\bar{1}$ 0)	0.44 nm
22.4	(0 2 0)	0.40 nm
26.6	(0 0 2)	0.34 nm
31.3	(100)	0.29 nm
33.2	(002)	0.27 nm
35.5	(101)	0.25 nm

The dissolution of native cellulose from orange peel (Cellulose I) in a NaOH/Urea system disrupts the highly ordered, crystalline hydrogen-bond network of the biomass. When this cellulose is regenerated into an aerogel, it often results in a less ordered, semi-crystalline structure known as

Cellulose II or a significant amorphous fraction. The transition from the crystalline Cellulose I (natural orange peel Fiber) to Cellulose II during dissolution and subsequent coagulation causes a loss of long-range periodic order, which manifests as broad peak areas rather than sharp reflections.

Cellulose I shows 14.8^0,16.2^0,22.4^0 peaks and cellulose II shows 12.9^0,20.2^0 and 22.4^0

Gelatine is a large, non-crystalline protein that typically produces broad diffraction signals due to its disordered molecular structure. In ZnCAG the gelatine matrix further contributes to the overall amorphous character of the aerogel.

The freeze-drying process preserves a 3D porous structure with fine fibrillar networks. This structural complexity and the high degree of random orientation of chains in the aerogel "walls" lead to broad peaks in XRD.

The citrus peel contains complex organic molecules (pectin, cellulose, flavonoids) that act as capping agents. If the sample is not calcined at a very high temperature, a broad peak at **26.4^0 to 26.6^0** appears, representing the (002) plane of carbon.

While the ZnO will produce sharp characteristic peaks (31.3^0,33.2^0,35.5^0), the underlying cellulose-gelatin matrix remains the dominant source of the broad background hump. The crystallinity index (Cr l) is calculated using segal equation.

$$CrI = (I_{002} - I_{amr}) \times 100 / I_{002}$$

Where $I_{002} = 1566.03$

$I_{amr} = 1251.87$

Then Cr I = 20.1 %

A 20.1% crystallinity index (CI) means that approximately one-fifth of the material's structure is highly ordered (crystalline), while the remaining four-fifths (around 79.9%) are disordered (amorphous).

The conformation from the XRD results the amorphous character of the ZnCAG, which is crucial for the sorption, porous structure and successful preparation of aerogel.

3.2 FTIR SPECTRUM OF PREPARED ZnCAG

FTIR spectroscopy was employed to study the changes in functional groups present in the raw orange peel and the resulting cellulose aerogel after chemical treatment and cross-linking. The spectrum confirmed the successful extraction of cellulose and its subsequent cross-linking with gelatine to form the aerogel matrix.

A normal orange peel cellulose aerogel shows broad absorption bands around 3200-3300cm^{-1} regions indicated the O–H stretching vibration, whereas the absorption peaks around 1600-1640 cm^{-1} showed the O–H bending of absorbed water.

The absorption peaks near 2900 cm^{-1} corresponded to the aliphatic C–H stretching vibration of all hydrocarbon constituents in polysaccharides. The peaks found on spectra at 1425-1428 cm^{-1} indicated CH_2 symmetric bending. Furthermore, the peaks in the regions around 1160 cm^{-1} were assigned to C–O–C asymmetrical ring stretching. while the peak at 896 cm^{-1} was contributed by the stretching of the β-glycosidic linkages of cellulose.*(1)*

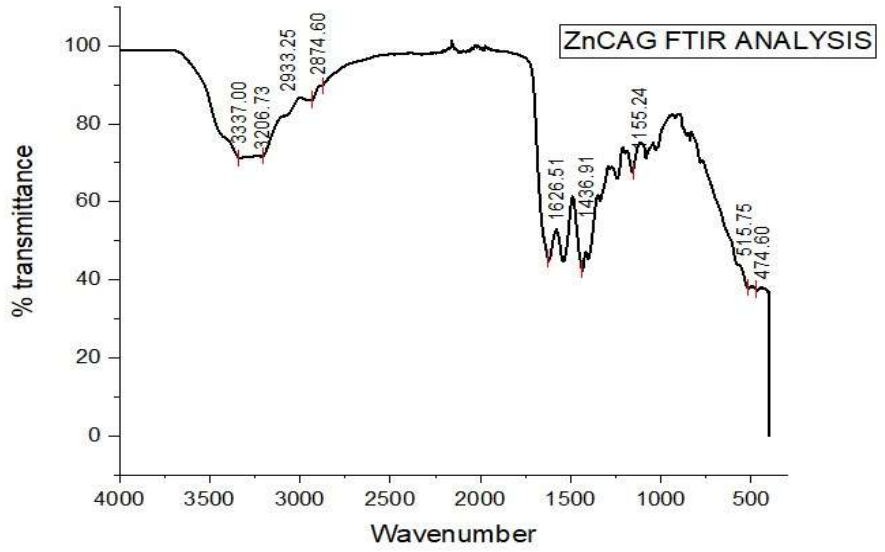

Fig.3.2.FTIR spectrum of ZnCAG

Fig.3.2 shows the FT-IR spectra of ZnCAG. A broad, intense peak characteristic of cellulose's extensive hydrogen-bonding network. The width indicates the presence of both intra- and intermolecular H-bonds. The peaks 3337.00cm^{-1} and 3206.73cm^{-1} show O-H stretching, broad and intense peak due to hydroxyl groups in cellulose and absorbed water. The 2933.25cm^{-1} and 2874.60cm^{-1} shows the C-H stretching peaks from the methyl and methylene groups of the cellulose structure. The peak at 1626.51cm^{-1}is often attributed to O-H bending of absorbed water. The peak 1436.91 cm^{-1} assigned to the CH_2 bending, crystallinity bond of cellulose expected at 1415-1430 cm^{-1} but slightly varied because of interactions with Zn compound. The 1155.24cm^{-1} peak shows the characteristic C-O-C and C-O-H stretching related to the saccharide structure of cellulose including the glycosidic ether linkage. 515.75 cm^{-1} and 474.60 cm^{-1} correspond to the stretching vibrations of the Zn-O bonds, distinct peaks in the far IR region confirm the presence and formation of the Zn-O bond.

The peak at 3337.00cm^{-1} clearly indicates the O-H stretching vibrational frequency and hydroxyl group, but the peak at 3206.73cm^{-1} showed a shift from the normal expected value can be evidenced as the interaction of Zn ions between the O-H groups in the cellulose matrix.

The clear appearance of the distinct peaks at 515.75 cm^{-1} and 474.60 cm^{-1} confirms the presence and formation of Zn-O bond in the cellulose structure.

3.3 MORPHOLOGY AND STRUCTURE OF THE AEROGEL

Aerogels are characterized by an open, highly porous, low density, and air-filled structure with high degree porosity and surface area *(45,46)*. They have very high adsorption capacities due to their peculiar properties*(46,47)*.

3.3.1 SCANNING ELECTRON MICROSCOPY

Fig.3.3 shows the SEM analysis of the non-doped cellulose aerogel. The non-doped sample exhibits a layered, flake-like morphology and it appears as a collection of randomly oriented, flat platelets or scales. There is a noticeable lack of a continuous 3D porous network. Instead, the cellulose appears somewhat aggregated or collapsed. The spaces between the flakes are irregular and do not represent the "honeycomb" structure typically sought in high-performance aerogels. It appears to be flatter and smooth surface. It shows a dense surface with smaller, shallower pores. The layers seem to be fused into a thicker matrix.

The Fig.3.4 shows the SEM image of ZnCAG. It reveals a highly 3D, irregular, and leafy structure with prominent flakes. There is large visible macropores between the layers The layers look distinct and loosely packed,

showing high surface area. The cellulose fibres are coated with granular ZnO particles.

The deposition of ZnO particles masks the hydrophilic hydroxyl groups of cellulose. This typically increases the water contact angle, making the aerogel hydrophobic and oleophilic—ideal for selectively absorbing oil while repelling water. The rough, particle-decorated surface increases the surface area available for oil film adhesion.(7).

Overall, the SEM morphology of Zn^{2+} doped cellulose aerogel shows enhanced adsorption and interaction applications.

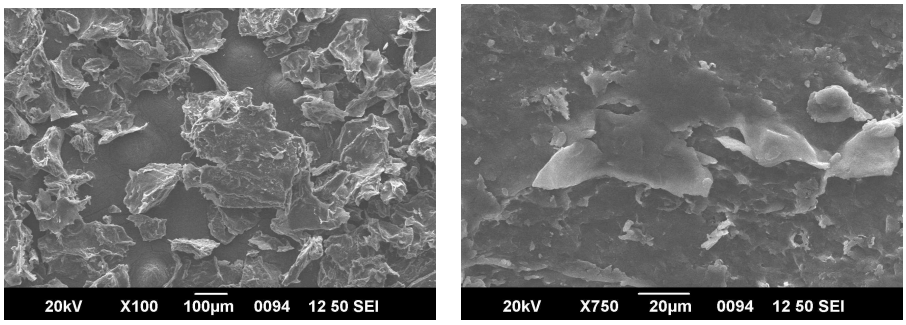

Fig 3.3.SEM images of non-doped cellulose aerogel

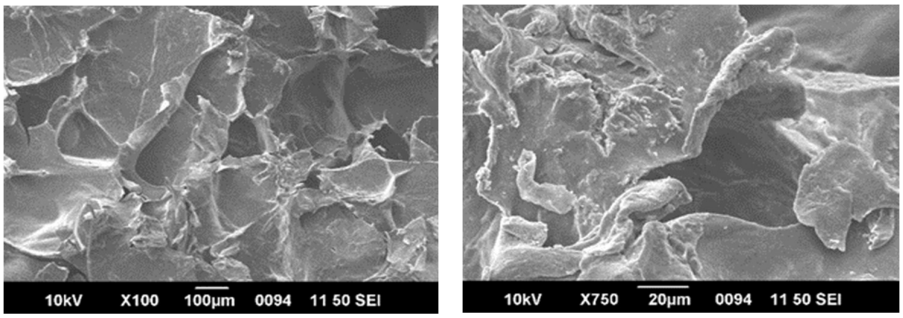

Fig 3.4.SEM images of Zn doped cellulose aerogel

3.3.2 ENERGY DISPERSIVE X-RAY ANALYSIS

Fig 3.6 shows the EDAX of ZnCAG. SEM-EDX is a powerful analytical technique that combines Scanning Electron Microscopy (SEM) for high-resolution surface imaging with Energy-Dispersive X-ray Spectroscopy (EDX) for elemental composition analysis. It allows for the simultaneous visualization of a sample's surface structure and the identification of its constituent elements, which is useful for fields like materials science, forensic investigation, and quality control, confirms the successful matrix and indicates a porous, stable composite structure suitable for sorption.

The EDAX spectrum confirms the elemental composition of the synthesized cellulose–gelatin/ZnO composite. Prominent peaks corresponding to carbon (C ~0.28 keV), nitrogen (N ~0.39 keV), and oxygen (O ~0.52 keV) are characteristic signals typically observed in biopolymeric matrices such as cellulose and gelatine, consistent with previously reported EDAX profiles of polysaccharide-based aerogels (as reported in cellulose aerogel studies).

A small peak for sodium (Na ~1.04 keV) suggests the presence of residual Na^+ ions originating from the NaOH–urea dissolution system, similar to earlier findings in regenerated cellulose prepared using alkaline–urea solvents (noted in NaOH–urea cellulose literature).

Distinct peaks for zinc (Zn Lα ≈ 1.0 keV, Zn Kα ≈ 8.6 keV, and Zn Kβ ≈ 9.6 keV) confirm the successful formation and incorporation of ZnO particles. These characteristic Zn peaks are in agreement with previously reported EDAX analyses of ZnO-loaded cellulose and other biopolymer composites (as documented in ZnO–biopolymer composite characterization studies).

Overall, the EDAX results validate the coexistence of the organic biopolymer framework and ZnO particles, confirming the successful synthesis of the ZnO–reinforced cellulose aerogel composite.

TABLE 3.5 shows the composition of ZnCAG

Element	Line Type	Wt%	Atomic %
C	K series	39.95	47.88
N	K series	17.92	18.41
O	K series	31.98	28.77
Na	K series	6.66	4.17
Zn	K series	3.5	0.77
Total:		100	100

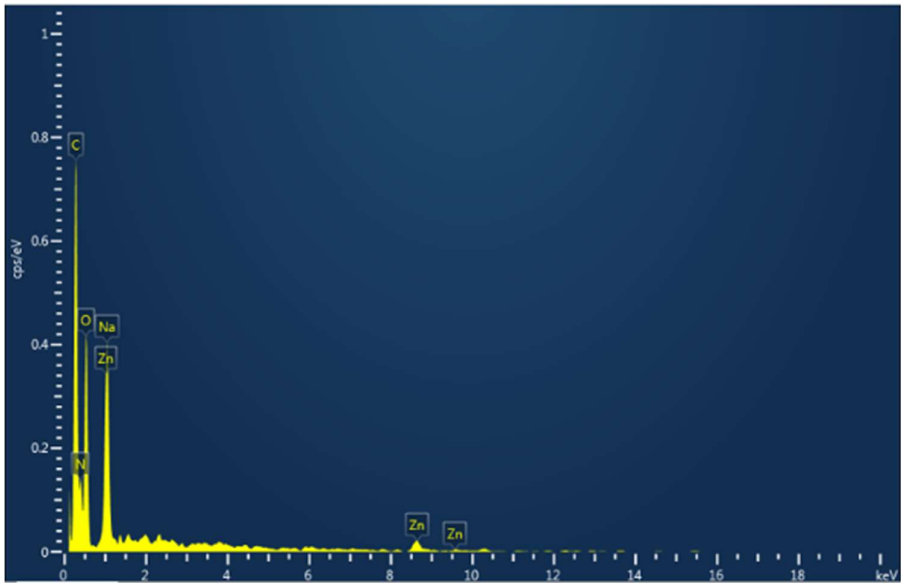

Fig.3.6. EDAX spectrum of ZnCAG

3.4 OIL ADSORPTION CAPACITY OF ZnCAG

Fig.3.7. shows the sorption of oil by Zn CAG.

Oil adsorption capacity of aerogel decreases with increase in concentration. The oil adsorption capacity (Q) was used to evaluate the efficiency of the aerogel template. The oil adsorption capacity was calculated as follows:*(42)*

$$Q= (W_1-W_0)/W_0$$

Where,

W_1 is the weight of the Zn CAG before sorption (0.43g),

W_0 is the weight of the Zn CAG after sorption (2.93g).

The ZnCAG shows Q (oil adsorption capacity) =5.814 g/g

An oil adsorption capacity of 5.824 g/g means that each gram of the Zn-doped cellulose aerogel can adsorb 5.824 grams of oil.

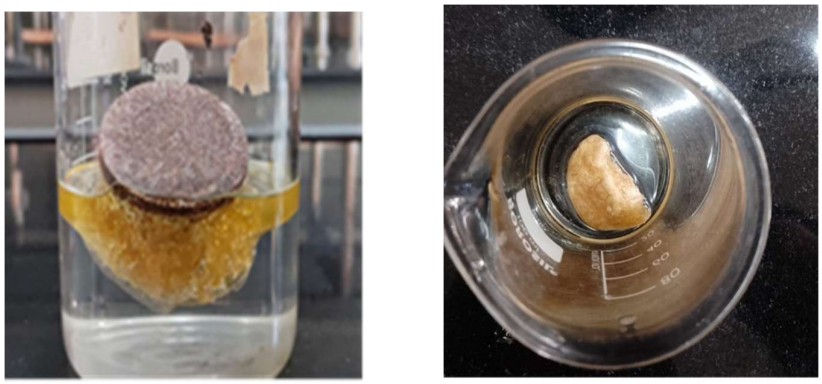

Fig.3.7. Oil sorption of ZnCAG

3.5 OIL REMOVAL EFFICIENCY OF Zn CAG

The oil removal efficiency was calculated using equation:*(42)*

$$RE\ (\%) = (W_1\text{-}W_0) \times 100/W_1$$

Where W_1 = weight of the ZnCAG after sorption (2.93)

W_0= weight of the ZnCAG before sorption (0.43)

The Zn CAG shows oil removal capacity RE (%) =85.32%.

It indicates how well the material works compared to 100% efficiency (removing all oil) or 0% efficiency (removing no oil). The efficiency value is specific to this particular material—a cellulose aerogel enhanced with zinc (Zn) doping. The addition of zinc is likely intended to improve the

material's sorption properties, reusability, or mechanical strength compared to a pure cellulose aerogel. Ultimately, 85.32% is a strong result within material science. It also shows high hydrophobic character of the prepared ZnCAG. Research suggesting that the developed material is effective for environmental oil spill remediation purposes.

Chapter 4

Conclusions

Agricultural and commercial waste streams present significant opportunities for sustainable material innovation. Among these, orange peel (Citrus sinensis) stands out as a particularly abundant and underutilized resource. While conventional applications focus primarily on essential oil extraction and cosmetic formulations, emerging research demonstrates far greater potential for value creation from this citrus byproduct.

This investigation centered on converting orange peel waste into a functional cellulosic aerogel material characterized by exceptional lightness and porosity. The synthesis pathway involved a systematic four-stage process: alkali-based treatment, cellulose isolation, aerogel formation with zinc acetate doping, and freeze-drying stabilization. This sequential approach effectively eliminated non-cellulosic components while incorporating zinc acetate as a dopant to enhance material properties.

A prepration done structural and compositional analysis was conducted using X-ray diffraction (XRD), Scanning electron microscopy (SEM), Electron dispersive X-ray analysis(EDAX/EDX) and Fourier-transform infrared spectroscopy (FTIR). SEM analysis showed an interconnected open-cell structure, providing the high surface area necessary for sorption. EDAX and FTIR confirmed successful ZnO particle incorporation within the porous matrix. XRD revealed a 20.1% crystallinity index indicates

amorphous structure (79.9%),better flexibility. The characterization results revealed that the zinc acetate-doped aerogel exhibits a highly porous morphology coupled with an amorphous structural arrangement and remarkably low bulk density, confirming successful transformation of the orange peel waste into a novel functional material.

Performance evaluation demonstrated that the ZnCAG achieved an oil adsorption capacity (Q) of 5.814g/g and an oil removal efficiency of 85.32%. Notably, adsorption capacity decreased with increasing zinc acetate concentration, highlighting the material's potential for oil spill remediation and wastewater treatment applications.

References

1. Ng wen yi, v.; ng, c. H.; peng, t. Y.; xian, o. Z.; hoong, s. S. Isolation of cellulose derived from orange peel and its application in biodegradable films. *Cellulose chemistry and technology* **2021**, *55*(3–4), 311–324. Doi:10.35812/cellulosechemtechnol.2021.55.31.

2. Otoni, c. G.; azeredo, h. M. C.; mattos, b. D.; beaumont, m.; correa, d. S.; rojas, o. J. The food–materials nexus: next generation bioplastics and advanced materials from agri-food residues (adv. Mater. 43/2021). *Advanced materials* **2021**, *33*(43). Doi:10.1002/adma.202170342.

3. Mat zain, n. F. Preparation and characterization of cellulose and nanocellulose from pomelo (citrus grandis) albedo. *Journal of nutrition & food sciences* **2014**, *05*(01). Doi:10.4172/2155-9600.1000334.

4. Chen, h. Chemical composition and structure of natural lignocellulose. In *biotechnology of lignocellulose*; springer netherlands: dordrecht, 2014; pp 25–71. Doi:10.1007/978-94-007-6898-7_2.

5. Long, l.-y.; weng, y.-x.; wang, y.-z. Cellulose aerogels: synthesis, applications, and prospects. *Polymers* **2018**, *10*(6), 623. Doi:10.3390/polym10060623.

6. Klemm, d.; heublein, b.; fink, h.; bohn, a. Cellulose: fascinating biopolymer and sustainable raw material. *Angewandte chemie international edition* **2005**, *44*(22), 3358–3393. Doi:10.1002/anie.200460587.

7. Kamal mohamed, s. M.; ganesan, k.; milow, b.; ratke, l. The effect of zinc oxide (zno) addition on the physical and morphological properties of cellulose aerogel beads. *Rsc advances* **2015**, *5*(109), 90193–90201. Doi:10.1039/c5ra17366c.

8. Feng, j.; nguyen, s. T.; fan, z.; duong, h. M. Advanced fabrication and oil absorption properties of super-hydrophobic recycled cellulose aerogels. *Chemical*

engineering journal **2015**, *270*, 168–175. Doi:10.1016/j.cej.2015.02.034.

9. Patra, n.; ramesh, p.; ţălu, ştefan. Advancements in cellulose-based materials for co2 capture and conversion. *Polymers* **2025**, *17*(7), 848. Doi:10.3390/polym17070848.

10. Li, Y., Liu, X., He, X., et al. (2023). MOF-Derived Co/C and mxene co-Decorated Cellulose-Derived Hybrid Carbon Aerogel with a Multi-Interface Architecture toward Absorption-Dominated Ultra-Efficient Electromagnetic Interference Shielding. ACS Applied Materials & Interfaces, 15(4), 5784–5796. Https://doi.org/10.1021/acsami.2c22447

11. Li, j.; li, j.; wang, g.; zhang, t.; dai, w.; ho, k. F.; et al. Molecular characteristics of organic compositions in fresh and aged biomass burning aerosols. *Science of the total environment* **2020**, *741*, 140247. Doi:10.1016/j.scitotenv.2020.140247.

12. Cao, j.; sun, g.; wang, p.; meng, c. Microstructured cnts/cellulose aerogel for a highly sensitive pressure sensor. *Acs applied materials & interfaces* **2024**, *16*(40), 54652–54662. Doi:10.1021/acsami.4c12566.

13. Pung, t.; ponglong, n.; panich-pat, t. Fabrication of pomelo-peel sponge aerogel modified with hexadecyltrimethoxysilane for the removal of oils/organic solvents. *Water, air, & soil pollution* **2022**, *233*(7), 283. Doi:10.1007/s11270-022-05766-8.

14. Zhu, l.; wang, y.; wang, y.; you, l.; shen, x.; li, s. An environmentally friendly carbon aerogels derived from waste pomelo peels for the removal of organic pollutants/oils. *Microporous and mesoporous materials* **2017**, *241*, 285–292. Doi:10.1016/j.micromeso.2016.12.033.

15. Tu, p. M.; vy, d. N. C.; ngan, l. T.; lam, c. V.; thang, t. Q.; duyen, n. H. K.; et al. Superhydrophobic banana stem–derived carbon aerogel for oil and organic adsorptions and energy storage. *Biomass conversion and biorefinery* **2024**, *14*(17), 20089–20103. Doi:10.1007/s13399-023-04176-y.

16. Muhammad, s.; albadn, y. M.; yahya, e. B.; nasr, s.; khalil, h. P. S. A.; ahmad, m. I.; et al. Trends in enhancing the efficiency of biomass-based aerogels for oil spill clean-up. *Giant* **2024**, *18*, 100249. Doi:10.1016/j.giant.2024.100249.

17. Yue, x.; zhang, t.; yang, d.; qiu, f.; li, z. Hybrid aerogels derived from banana peel and waste paper for efficient oil absorption and emulsion separation. *Journal of cleaner production* **2018**, *199*, 411–419. Doi:10.1016/j.jclepro.2018.07.181.

18. Luu, t. P.; do, n. H. N.; chau, n. D. Q.; lai, d. Q.; nguyen, s. T.; le, d. K.; et al. Morphology control and advanced properties of bio-aerogels from pineapple leaf waste. *Chemical engineering transactions* **2020**, *78*, 433–438. Doi:10.3303/cet2078073.

19. Do, n. H. N.; tran, v. T.; tran, q. B. M.; le, k. A.; thai, q. B.; nguyen, p. T. T.; et al. Recycling of pineapple leaf and cotton waste fibers into heat-insulating and flexible cellulose aerogel composites. *Journal of polymers and the environment* **2021**, *29*(4), 1112–1121. Doi:10.1007/s10924-020-01955-w.

20. Do, n. H. N.; truong, b. Y.; nguyen, p. T. X.; le, k. A.; duong, h. M.; le, p. K. Composite aerogels of tempo-oxidized pineapple leaf pulp and chitosan for dyes removal. *Separation and purification technology* **2022**, *283*, 120200. Doi:10.1016/j.seppur.2021.120200.

21. Dai, y.; jing, z.; qiu, z.; zhu, y.; qiu, f.; pan, j.; et al. Multifunctional biomass carbon fiber aerogel based on resource utilization of agricultural waste-peanut shells for fast and efficient oil–water/emulsion separation. *Materials science and engineering: b* **2022**, *283*, 115819. Doi:10.1016/j.mseb.2022.115819.

22. Dai, q.; li, d.; sun, y.; wang, h.; lu, y.; yang, d. Low temperature-resistant superhydrophobic and elastic cellulose aerogels derived from seaweed solid waste as efficient oil traps for oil/water separation. *Chemosphere* **2023**, *336*, 139179. Doi:10.1016/j.chemosphere.2023.139179.

23. Chhajed, m.; verma, c.; sathawane, m.; singh, s.; maji, p. K. Mechanically durable green aerogel composite based on agricultural lignocellulosic residue for

organic liquids/oil sorption. *Marine pollution bulletin* **2022**, *180*, 113790. Doi:10.1016/j.marpolbul.2022.113790.

24. Dilamian, m.; noroozi, b. Rice straw agri-waste for water pollutant adsorption: relevant mesoporous super hydrophobic cellulose aerogel. *Carbohydrate polymers* **2021**, *251*, 117016. Doi:10.1016/j.carbpol.2020.117016.

25. Tran, d. T.; nguyen, s. T.; do, n. D.; thai, n. N. T.; thai, q. B.; huynh, h. K. P.; et al. Green aerogels from rice straw for thermal, acoustic insulation and oil spill cleaning applications. *Materials chemistry and physics* **2020**, *253*, 123363. Doi:10.1016/j.matchemphys.2020.123363.

26. Huang, j.; li, d.; huang, l.; tan, s.; liu, t. Bio-based aerogel based on bamboo, waste paper, and reduced graphene oxide for oil/water separation. *Langmuir* **2022**, *38*(10), 3064–3075. Doi:10.1021/acs.langmuir.1c02821.

27. Wu, j.; dong, y.; xu, m.; xia, j.; liu, z.; cao, y. Aerogels made from soybean stalk with various lignocellulose aggregating states for oil spill clean-up. *Cellulose* **2021**, *28*(15), 9873–9891. Doi:10.1007/s10570-021-04146-5.

28. Kumar, g.; dora, d. T. K.; jadav, d.; naudiyal, a.; singh, a.; roy, t. Utilization and regeneration of waste sugarcane bagasse as a novel robust aerogel as an effective thermal, acoustic insulator, and oil adsorbent. *Journal of cleaner production* **2021**, *298*, 126744. Doi:10.1016/j.jclepro.2021.126744.

29. Septiani, e. L.; prastuti, o. P.; kurniati, y.; fauziyah, m.; widiyastuti, w.; setyawan, h.; et al. Sorption efficiency in dye removal and thermal stability of sorghum stem aerogel. *Materials science forum* **2019**, *966*, 175–180. Doi:10.4028/www.scientific.net/msf.966.175.

30. Xing, h.; fei, y.; cheng, j.; wang, c.; zhang, j.; niu, c.; et al. Green preparation of durian rind-based cellulose nanofiber and its application in aerogel. *Molecules* **2022**, *27*(19), 6507. Doi:10.3390/molecules27196507.

31. Shi, g.; qian, y.; tan, f.; cai, w.; li, y.; cao, y. Controllable synthesis of pomelo peel-based aerogel and its application in adsorption of oil/organic pollutants.

Royal society open science **2019**, *6*(2), 181823. Doi:10.1098/rsos.181823.

32. Chaudhary, s.; dora, d. T. K.; porwal, s. K. Silicon-free psma-modified aerogel derived from waste fruit peels for efficient oil recovery. *Biomass conversion and biorefinery* **2024**, *14*(23), 29659–29671. Doi:10.1007/s13399-023-04720-w.

33. Phat, l. N.; nguyen, h. C.; khoa, b. D. D.; khang, p. T.; tien, d. X.; thang, t. Q.; et al. Synthesis and surface modification of cellulose cryogels from coconut peat for oil adsorption. *Cellulose* **2022**, *29*(4), 2435–2447. Doi:10.1007/s10570-022-04427-7.

34. Nguyen, h. M.; tran, k. A.; nguyen, t. T. N.; do, n. N. H.; le, k. A.; le, p. K. Fabrication of carbon aerogels from coir for oil adsorption. *Iop conference series: earth and environmental science* **2022**, *964*(1), 012033. Doi:10.1088/1755-1315/964/1/012033.

35. Cai, t.; wang, h.; jin, c.; sun, q.; nie, y. Fabrication of nitrogen-doped porous electrically conductive carbon aerogel from waste cabbage for supercapacitors and oil/water separation. *Journal of materials science: materials in electronics* **2018**, *29*(5), 4334–4344. Doi:10.1007/s10854-017-8381-5.

36. Imran, m.; islam, a.; farooq, m. U.; ye, j.; zhang, p. Characterization and adsorption capacity of modified 3d porous aerogel from grapefruit peels for removal of oils and organic solvents. *Environmental science and pollution research* **2020**, *27*(35), 43493–43504. Doi:10.1007/s11356-020-09085-5.

37. Bunaciu, a. A.; udriştioiu, e. Gabriela; aboul-enein, h. Y. X-ray diffraction: instrumentation and applications. *Critical reviews in analytical chemistry* **2015**, *45*(4), 289–299. Doi:10.1080/10408347.2014.949616.

38. Role of surfactants and polymers for clay minerals as stabilizer of pickering emulsion; 2022; pp 277–314. Doi:10.1016/b978-0-323-91858-9.00007-0.

39. Xiao, k.; xu, y.; cao, x.; xu, h.; li, y. Advanced characterization of membrane surface fouling. In *60 years of the loeb-sourirajan membrane*; elsevier, 2022; pp

499–532. Doi:10.1016/b978-0-323-89977-2.00022-1.

40. Neikov, o. D.; yefimov, n. A. Powder characterization and testing. In *handbook of non-ferrous metal powders*; elsevier, 2019; pp 3–62. Doi:10.1016/b978-0-08-100543-9.00001-4.

41. Gupta, b. D.; semwal, v.; pathak, a. Nanotechnology-based fiber-optic chemical and biosensors. In *nano-optics*; elsevier, 2020; pp 163–195. Doi:10.1016/b978-0-12-818392-2.00007-x.

42. Ratcha, a.; samart, c.; yoosuk, b.; sawada, h.; reubroycharoen, p.; kongparakul, s. Polyisoprene modified poly(alkyl acrylate) foam as oil sorbent material. *Journal of applied polymer science* **2015**, *132*(42). Doi:10.1002/app.42688.

43. Anovitz, l. M.; cole, d. R. Characterization and analysis of porosity and pore structures. *Reviews in mineralogy and geochemistry* **2015**, *80*(1), 61–164. Doi:10.2138/rmg.2015.80.04.

44. Franco, p.; cardea, s.; tabernero, a.; de marco, i. Porous aerogels and adsorption of pollutants from water and air: a review. *Molecules* **2021**, *26*(15), 4440. Doi:10.3390/molecules26154440.

45. Nita, l. E.; ghilan, a.; rusu, a. G.; neamtu, i.; chiriac, a. P. New trends in bio-based aerogels. *Pharmaceutics* **2020**, *12*(5), 449. Doi:10.3390/pharmaceutics12050449.

46. Qiu, j.; guo, x.; lei, w.; ding, r.; zhang, y.; yang, h. Facile preparation of cellulose aerogels with controllable pore structure. *Nanomaterials* **2023**, *13*(3), 613. Doi:10.3390/nano13030613.

47. Chen, x.; chen, j.; you, t.; wang, k.; xu, f. Effects of polymorphs on dissolution of cellulose in naoh/urea aqueous solution. *Carbohydrate polymers* **2015**, *125*, 85–91. Doi:10.1016/j.carbpol.2015.02.054.